ELSEVIER

Contents lists available at ScienceDirect

# Experimental Eye Research

journal homepage: www.elsevier.com/locate/yexer



Short communication

# Subtle retinal degeneration in pigmented *Abca4*<sup>-/-</sup> *Rdh8*<sup>-/-</sup> mice

Sarah Glänzer, Josef Biber, Antje Grosche

Department of Physiological Genomics, Biomedical Center, Ludwig-Maximilians-Universität München, Germany

#### ABSTRACT

Stargardt disease type 1 is a genetic retinal disorder caused by mutations in the ABCA4 gene, leading to toxic bisretinoid accumulation in the retinal pigment epithelium (RPE). This study examines the retinal phenotype of  $Abca4^{-/-}$  Rdh8 $^{-/-}$  double knockout mice on a C57BL/6J background, excluding confounding variants such as the Rpe65 Leu450Met variant or the rd8 mutation in the Crb1 gene, to define the effect of combined Abca4 and Rdh8 deficiency.

Double knockout mice—confirmed free of the rd8 mutation and to not carry the protective Met variant of the Rpe65 gene—were analyzed at 4 and 9 months and compared to  $Rdh8^{-/-}$  single knockouts under varying light exposure. Histological assessments included RPE autofluorescence, morphometric parameters of microglial activation, and retinal layer integrity.

At 4 months, no significant structural differences were observed between genotypes. By 9 months,  $Abca4^{-/-}$  Rdh8<sup>-/-</sup> mice showed increased RPE autofluorescence, consistent with elevated bisretinoid accumulation. Four-fold enhanced light exposure affected microglial morphology, and a modest age-related thinning of retinal layers was noted in double knockouts.

In conclusion, increased RPE autofluorescence was confirmed in  $Abca4^{-/-}$   $Rdh8^{-/-}$  mice on the C57BL/6J background, but only mild retinal structural and inflammatory changes were observed. The severe early-onset degeneration reported in prior studies was not replicated, likely due to the absence of the rd8 mutation present in the double knockout mouse strain at its original description. This suggests that the rd8 mutation drove neurodegeneration, while the combined Abca4 and Rdh8 deficiency alone is comparatively well tolerated in the murine retina.

# 1. Introduction

Stargardt disease type 1 is a retinal disorder predominantly inherited in an autosomal recessive manner and classified within the group of macular dystrophies. It often manifests during adolescence with varying degrees of visual acuity impairment and central scotomas (Genead et al., 2009). The disease typically leads to a loss of central visual acuity, while peripheral vision generally remains unaffected (Genead et al., 2009). In the early stages, funduscopic examination reveals central irregularities in pigmentation, followed by progressive atrophy characterized by yellowish-gray spots that gradually coalesce in the macular region (Stargardt, 1909, 1913, 1916). This specific alteration is referred to as fundus flavimaculatus (Rudolph et al., 2002). The disease typically manifests before the age of 20 and is most commonly associated with a mutation in the *ABCA4* (ATP-binding cassette subfamily A member 4) gene (Allikmets et al., 1997).

ABCA4 is a retina-specific ATP-binding cassette transporter that facilitates the translocation of all-trans-retinal—produced via photo-isomerization of 11-cis-retinal—across photoreceptor outer segment disc membranes into the cytoplasm (Allikmets et al., 1997; Sun and Nathans, 1997; Molday et al., 2000). In the cytoplasm, all-trans-retinal is reduced to all-trans-retinol (atROL) by retinol dehydrogenase 8 (RDH8),

which catalyzes the first step in the visual cycle's regeneration of 11-cis-retinal (Kiser et al., 2014; Arrigo et al., 2025). The retinal pigment epithelium (RPE), located beneath the neuroretina and in direct contact with photoreceptor outer segments, plays a central role in the visual cycle. It also expresses ABCA4, albeit at much lower levels than photoreceptor outer segments (Molday et al., 2018), takes up atROL from photoreceptors, and completes the conversion of the latter back into 11-cis-retinal. This is then returned to photoreceptors to sustain light sensitivity (Choi et al., 2021). In healthy photoreceptors, all-trans-retinal released after photoisomerization can react with phosphatidylethanolamine (PE) in the disc membranes to form N-retinylidene-PE, which is then flipped to the cytoplasmic leaflet by the ATP-binding cassette transporter ABCA4 and reduced to atROL. In Stargardt disease, loss-of-function mutations in ABCA4 impair this transport step, trapping N-retinylidene-PE within the disc lumen. This promotes secondary condensation reactions between all-trans retinal yielding bisretinoid adducts such as nylidene-N-retinylethanolamine (A2E) (Choi et al., 2021). These bisretinoids are non-enzymatically formed, cannot be degraded by lysosomal enzymes, and are transferred to the RPE during daily phagocytosis of photoreceptor outer segment discs. Over time, they accumulate within RPE lysosomes as lipofuscin, which exhibits strong autofluorescence

E-mail address: Antje.Grosche@med.uni-muenchen.de (A. Grosche).

<sup>\*</sup> Corresponding author.

detectable by fundus autofluorescence imaging in patients with Stargardt's disease (Burke et al., 2014). The buildup of bisretinoid lipofuscin is toxic to RPE cells through mechanisms including phototoxic reactive oxygen species generation, disruption of lysosomal function, and complement activation, ultimately contributing to photoreceptor degeneration in Stargardt disease (Burke et al., 2014). In line with this, previous studies have shown that bisretinoid fluorophores (e.g. N-retinylidene-N-retinylethanolamine (A2E)) accumulate in the RPE of both pigmented and albino *Abca4*<sup>-/-</sup> single knockout mice, accompanied by increased oxidative stress, inflammation, and complement activation at the level of RPE, but little neurodegeneration (Radu et al., 2011; Charbel Issa et al., 2013; Jabri et al., 2020). Consistent with this, even stronger elevations of A2E and retinaldehyde dimers (RALdi) levels in an Abca4<sup>-/-</sup> Rdh8<sup>-/-</sup> double knockout strain have been reported (Maeda et al., 2008; Kiser et al., 2014). Additionally to that and in contrast to the Abca4<sup>-/-</sup> single knockout mice, Maeda et al. reported regional neurodegeneration as early as 4-6 weeks, which manifested after 3 months as reduced photoreceptor layer thickness, rosette formation and cell count (Maeda et al., 2008). By 5 months, only 4-6 rows of disorganized photoreceptors were detectable, and by 12 months, no cells of the ONL survived (Maeda et al. 2008, 2009; Shiose et al., 2011; Chen et al., 2012). Overall, the  $Abca4^{-/-}$   $Rdh8^{-/-}$  double knockout therefore seems to better phenocopy the pathology observed in Stargardt patients than the single knockouts (neither Abca4 nor Rdh8 knockouts show major signs of neurodegeneration), making it a potentially valuable mouse model for Stargardt-related research also in light of therapy development that could potentially also be of benefit for patients suffering from age-related macular degeneration.

Noteworthy, Maeda and colleagues mention the presence of the rd8 mutation in their mouse strain in addition to ABCA4 and RDH8 deficiency, in a study from 2013 (Chen et al., 2013), but most likely this holds true for the older work as well (Maeda et al. 2008, 2009; Shiose et al., 2011; Chen et al., 2012). This mutation in the Crb1 gene does not cause a complete knockout, but rather a frameshift mutation that severely disrupts the function of the resulting truncated CRB1 protein leading to rosette formation and focal photoreceptor degeneration particularly in the inferior-nasal regions of the retina at timelines similar to that initially also described for the Abca4<sup>-/-</sup> Rdh8<sup>-/-</sup> double knockout mice (Mehalow et al., 2003; Mattapallil et al., 2012). This suggests that the extensive retinal degeneration described in the early studies characterizing the Abca4<sup>-/-</sup> Rdh8<sup>-/-</sup> mice is likely due to this additional inbred rd8 mutation rather than the combined absence of functional ABCA4 and RDH8 (Maeda et al., 2008). Although recent studies have examined very young (4-week-old) *Abca4*<sup>-/-</sup> *Rdh8*<sup>-/-</sup> mice free of the potentially confounding rd8 mutation under light damage paradigms (Parmar et al. 2016, 2018; Schur et al., 2018; Yu et al., 2021), a systematic natural history study characterizing the phenotype in older mice remains lacking.

Here, we re-characterized the retinal structure and RPE autofluorescence in Abca4<sup>-/-</sup> Rdh8<sup>-/-</sup> double knockout mice on a C57BL/6J background free of the rd8 mutation (Jackson Laboratories, strain #030503). Note that we made sure that the animals were carrying the original Leucine 450 variant of the Rpe65 gene which renders them more light sensitive as compared to animals carrying the Leu450Met variant (Danciger et al., 2000; Kim et al., 2004). RPE65 is another protein of the visual cycle, playing a crucial role in rhodopsin regeneration primarily expressed by the RPE (Kim et al., 2004). The formation of bisretinoids and lipofuscin is particularly dependent on a functional visual cycle and proper chromophore regeneration (Kim et al., 2004). Rpe65<sup>-/-</sup> mice exhibit minimal lipofuscin deposits in the RPE during the aging process (Katz and Redmond, 2001). The Leu450Met variant appears to slow the enzyme's kinetics, resulting in reduced bisretinoid accumulation in the RPE (Kim et al., 2004) and increased tolerance to light-induced damage (Wenzel et al., 2001), protecting photoreceptors from excessive stress due to continuous phototransduction (Danciger et al., 2000). Histological assessments were performed on samples collected from four- and

nine-month-old mice. These efforts aimed to clarify the impact of combined ABCA4 and RDH8 deficiencies and provide a natural history study of this popular murine model of Stargardt disease, which was now confirmed to be free of the rd8 mutation.

#### 2. Methods

All animals were housed under a regular 12-h light/dark cycle with free access to water and food, in climate-controlled, pathogen-free facilities. All experiments were conducted in compliance with the German Animal Welfare Act. Experiments were performed on knockout mice with the genotypes  $Rdh8^{-/-}$  and  $Abca4^{-/-}$   $Rdh8^{-/-}$  on a C57BL/6J background (Jackson Laboratories, strain number #030503) at the ages of 4 and 9 months. A subset of these animals was exposed to higher light intensity between the fifth and ninth months of life by placing their cages on the top shelves of the mouse racks, where light levels were approximately four times greater (190 lux) than on the bottom shelves (45 lux). Prior to this period, all mice were housed under lower light conditions, consistent with standard procedures in the animal facility.

Genotyping of the mice was performed with the KAPA Mouse Genotyping Hot Start Kit (Merck, Darmstadt, Germany) using primers for Abca4 (forward: 5' AAGAGAAGCAATCAAATCAGGA 3'; reverse 1: 5' GAAGATGCTCTGGATATC TCT GC 3'; reverse 2: 5' TGAGTAGGTGT-CATTCTATTC TGG 3') Rdh8 (forward 1: 5' CACAACATCCCAGCACTCTG 3'; forward 2: 5' AGA CTG CCT TGG GAA AAG CG 3'; reverse: 5' ACTCCGCCTTGGAAACCTG 3'), rd1 (forward 1: 5' AAG CTA GCT GCA GTA ACG CCA TT 3'; forward 2: 5' ACC TGC ATG TGA ACC CAG TAT TC; reverse 1: 5' CTA CAG CCC CTC TCC AAG GTT TA 3'), rd8 (forward 1: 5' GGT GAC CAA TCT GTT GAC AAT CC 3'; reverse 1: 5' GCC CCA TTT GCA CAC TGA TG AC 3'), and Rpe65 (forward: 5' ACCA-GAAATTTGGAGGGAAAC 3'; reverse: 5' CCCTTCCATTCAGAGCTTCA 3'). For genotyping of Rpe65 Leu450Met polymorphism a protocol as published recently was used (Wenzel et al., 2001). Briefly, the PCR-amplified DNA was digested with the MwoI restriction enzyme (New England Biolabs) and analyzed on 2 % agarose gels. The sequence variant corresponding to the Met-450 variant produced distinct fragments of 180 and 365 bp due to the presence of the MwoI restriction site. In contrast, the Leu-450 codon abolishes the MwoI site, resulting in undigested or partially digested products, which were interpreted as indicative of homozygosity or heterozygosity for Leu-450, respectively.

For morphometric analysis on retinal sections, mouse eyes were fixed in 4 % PFA for 1 h. Note that during enucleation, the superior part of the eve and retina was marked by an incision enabling to trace back retinal subregions during experiments. After fixation, eyes were incubated in sucrose (30 % w/v in PBS) for cryoprotection, embedded in OCT compound and cut into sections of 20 µm thickness using a cryostat. For cryosectioning, the eye bulbs were oriented to include both the superior and inferior regions of the retina equidistant from the optic nerve within the same section. After thawing, drying and rehydrating the sections, tissue permeabilization was achieved by applying 0.2 % Triton X in PBS for 10 min, followed by three 10-min washes with PBS. For labelling of microglia, sections were incubated with the primary rabbit  $\alpha$ -IBA-1 antibody solution (1:500 dilution, Wako Chemicals, Neuss, Germany, cat. no. 019-19741) overnight at 4 °C, while the secondary donkey antirabbit antibody (Cy5-conjugated) solution (1:500 dilution, dissolved in PBS with 3 % BSA and 0.1 % Tween; Dianova (Hamburg, Germany, cat. no. 711-175-152) was applied for 2 h at room temperature. After three washes in PBS, 4,6-diamidino-2-phenylindole (DAPI, Sigma-Aldrich) was added in a 1:1000 dilution in PBS for 10 min at room temperature, followed by three additional 10-min washes with PBS. The slides were stored in the dark until analysis using a confocal microscope (custom-made VisiScope CSU-X1 confocal system equipped with highresolution sCMOS camera; Visitron Systems, Puchheim, Germany). To quantify subretinal microglia, we counted IBA + cells in the subretinal space of four central sections, each running through the optic nerve, from each mouse and calculated the mean for each animal. This value is plotted as a biological replicate in the respective graph. Measurements of retinal layer thickness were performed on retinal sections using the Fiji measurement tools.

For retinal and RPE wholemounts, the retinae or RPE were flattened with six radial cuts and transferred to 24-well plates for staining. The primary rabbit α-IBA-1 antibody solution (1:500 dilution, Wako Chemicals, Neuss, Germany, cat. no. 019-19741) was incubated overnight at 4 °C, while the secondary donkey anti-rabbit antibody (Cy5-conjugated) solution (1:500 dilution, dissolved in PBS with 3 % BSA and 0.1 %Tween; Dianova (Hamburg, Germany, cat. no. 711-175-152) was applied for 2 h at room temperature on a shaker. For RPE autofluorescence measurements, RPE wholemounts were excited with a 488 nm laser using a confocal microscope, and a z-projection of the resulting stack was generated. Three separate areas were scanned from each RPE wholemount per animal. Each area was located at an equal distance  $(\sim 200-300 \, \mu m)$  from the optic nerve head, if possible. The average pixel intensity was measured at using ImageJ software. The mean of these technical replicates was then plotted as one data point per animal, which was considered one biological replicate. To assess microglial morphology, the soma and endpoints of the processes were circled in the images, and the area circumscribed by these (soma area/occupied area) was calculated using Fiji (Schindelin et al., 2012). Up to ten microglial cells per image stack were analyzed for soma and total cell size, unless fewer cells were present in the stack. Three image stacks were obtained from retinal flatmounts per animal.

Data were analyzed using GraphPad PRISM 8 software, with results presented as mean  $\pm$  standard error. Statistically significant differences were determined using the Mann-Whitney U test.

#### 3. Results and discussion

For our re-characterization of  $Abca4^{-/-}$   $Rdh8^{-/-}$  mice that were confirmed to be free from rd1 or rd8 mutations, we first studied the agedependent rise in RPE autofluorescence as a major hallmark of the murine Stargardt model. Testing RPE autofluorescence in animals kept under normal light conditions, we found little difference between Rdh8<sup>-/-</sup> single-knockout and Abca4<sup>-/-</sup> Rdh8<sup>-/-</sup> double-knockout animals at 4 months of age (Fig. 1A). From this age onward, animals were housed either in the bottom row of the rack with minimal light exposure (~45 lux, hereafter referred to as low light exposure) or in the top row with 4-fold higher light exposure (~190 lux, hereafter referred to as high light exposure). Under high light exposure, 9-month-old animals of both genotypes exhibited a significant age-dependent increase in autofluorescence, but no genotype-dependent differences (Fig. 1A). Under low light exposure, RPE flatmounts from 9-month-old Abca4<sup>-/-</sup> Rdh8<sup>-/-</sup> double-knockout animals showed a trend (p = 0.1) toward higher autofluorescence intensity compared to age-matched  $Rdh8^{-/-}$  animals. Additionally, the relative age-dependent increase was more pronounced in *Abca4*<sup>-/-</sup> *Rdh8*<sup>-/-</sup>mice, with a fold change of up to 2.6, compared to 1.5 in  $Rdh8^{-/-}$  mice. These findings – especially those performed under low light conditions - align with what was originally found also in the Abca4<sup>-/-</sup> Rdh8<sup>-/-</sup> double-knockout stain that in addition carried the rd8 mutation (Maeda et al., 2008; Kiser et al., 2014). However, moderately increased light exposure also promotes buildup of autofluorescent material in RPE of  $Rdh8^{-/-}$  mice.

Following injury, microglia transition through various activation states, which are partially also reflected in distinct morphological changes. In their homeostatic state, they exhibit a highly ramified morphology, characterized by small somata and long, extensively branched processes. Under acute or chronic stress, these processes retract toward the cell body, which then adopts a rounded, amoeboid shape (Stence et al., 2001; Walker et al., 2013; Paolicelli et al., 2022). In this activated state, microglial somata enlarge, while the total area occupied by their processes decreases (Fig. 1B and C). When inflammation is resolved and a new tissue immune homeostasis is established, microglia may subsequently extend new, shorter processes (Stence et al.,

2001). Previous studies on  $Abca4^{-/-}$  single-knockout mice in the CD1 albino background revealed an increased number of microglial cells accompanied by a reduction in total microglial area compared to wild-type animals, particularly in the inner retinal layers (Jabri et al., 2020). Based on these expected morphological changes, we also assessed microglial activation in our double-knockout model determining the following parameters in retinal flatmounts stained for IBA1 delineating microglia and macrophages: the number of microglia per scan field (Fig. 1B), soma area, and the total area occupied by microglia and their processes (Fig. 1C). These parameters were assessed separately for the inner retina (ganglion cell layer to inner nuclear layer) and outer retina (outer plexiform layer to subretinal space). Notably, microglia in the outer retinal layers were fewer in number and exhibited a more highly ramified, potentially less activated morphology compared to those in the inner retina. At 4 months of age, no significant genotype-dependent differences were observed for any of these parameters. The only significant difference was detected in 9-month-old mice exposed to high light intensities: specifically, Abca4<sup>-/-</sup> Rdh8<sup>-/-</sup> mice exhibited fewer microglia in the inner retina compared to  $Rdh8^{-/-}$  mice. This might be due to increasing migration of microglia into the subretinal space – a site of inflammation because of stressed RPE in this mouse model as also indicated by the pattern of autofluorescence in aging mice and SLO images (Kohno et al., 2014). However, quantification of IBA1-positive cells along the full length of central eye sections from mice of both genotypes revealed only very few subretinal cells. No genotype-dependent differences could be detected (Fig. 1C). Additionally, Abca4<sup>-/-</sup> Rdh8<sup>-/</sup> mice showed a significant, age-dependent increase in microglial soma area in both the inner and outer retinal layers, indicating the onset of microglial activation (Fig. 1D). In contrast, no such changes were observed in  $Rdh8^{-/-}$  mice in either retinal layer. This supports findings from earlier findings in rd8 mutation free Abca4<sup>-/-</sup> Rdh8<sup>-/-</sup> mice that demonstrate low-grade chronic inflammation driven by microglia as deduced from chemokine profiling in aging mice under room light conditions or after bright light exposure (Kohno et al., 2014; Maeda et al., 2014; Palczewska et al., 2016). Please note that in all these studies, wild type animals and not  $Rdh8^{-/-}$  mice served as controls and in most cases, animals were younger than four months of age at the time point of the analysis.

Regarding the total area occupied by microglial processes, a significant reduction—approximately one-third of the initial value—was observed in both genotypes when comparing 9-month-old mice to their 4-month-old counterparts (Fig. 1D). This suggests that aging has a strong effect on this parameter, while genotype exerts only a minor influence. However,  $Abca4^{-/-}$   $Rdh8^{-/-}$  mice exhibited a more pronounced reorganization of microglial processes, particularly under low light conditions in the inner retina, where the total area decreased to one-quarter of the initial value (Fig. 1C). Despite these differences in process reorganization, no significant difference was observed in the area occupied by microglial processes between the two genotypes. Potentially, the subtle stress also present in the  $Rdh8^{-/-}$  single knockouts is sufficient to drive age-dependent microglial changes – a hypothesis that be considered and validated in future studies.

Maeda et al., 2008 reported an early onset of retinal degeneration in  $Abca4^{-/-}$   $Rdh8^{-/-}$  double knockout mice that however were also homozygous for the rd8 mutation. Given the predominant photoreceptor localization, the ABCA4-related pathology is expected to manifest primarily in the outer retina—namely the outer nuclear layer (ONL) and outer plexiform layer (OPL)—once photoreceptor loss, including degeneration of synaptic terminals, occurs. Consistently, a reduced ONL thickness and decreased photoreceptor nuclei count as early as three months of age was reported in  $Abca4^{-/-}$   $Rdh8^{-/-}$  double knockout mice (Maeda et al., 2008). Other studies have documented degeneration of the ONL beginning at 8 months (Wu et al., 2010) and degeneration of the ganglion cell layer (GCL) after 6 months in  $Abca4^{-/-}$  albino mice (Jabri et al., 2020). Given that Maeda et al. found an even more pronounced degeneration in the central inferior compared to the superior retinal

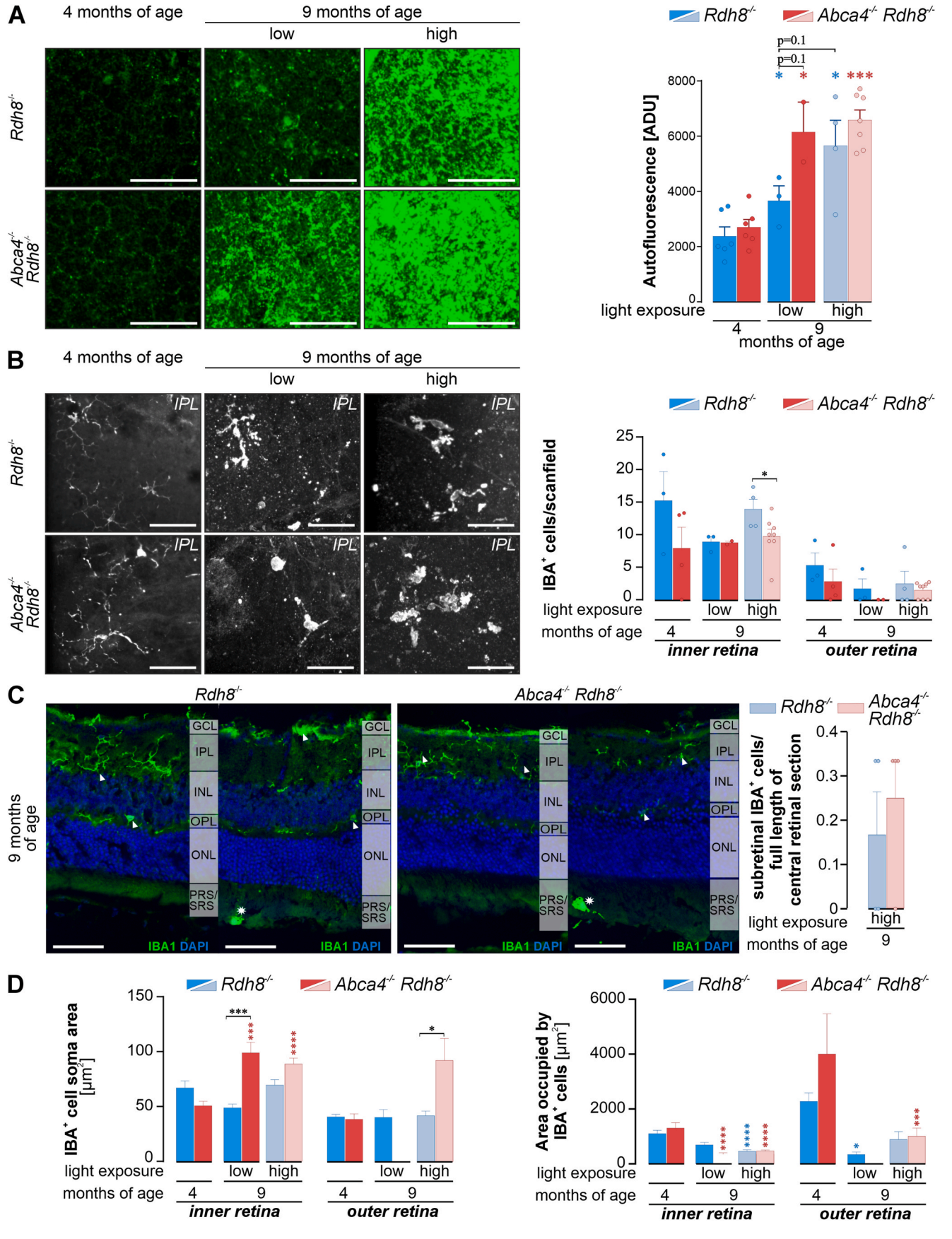


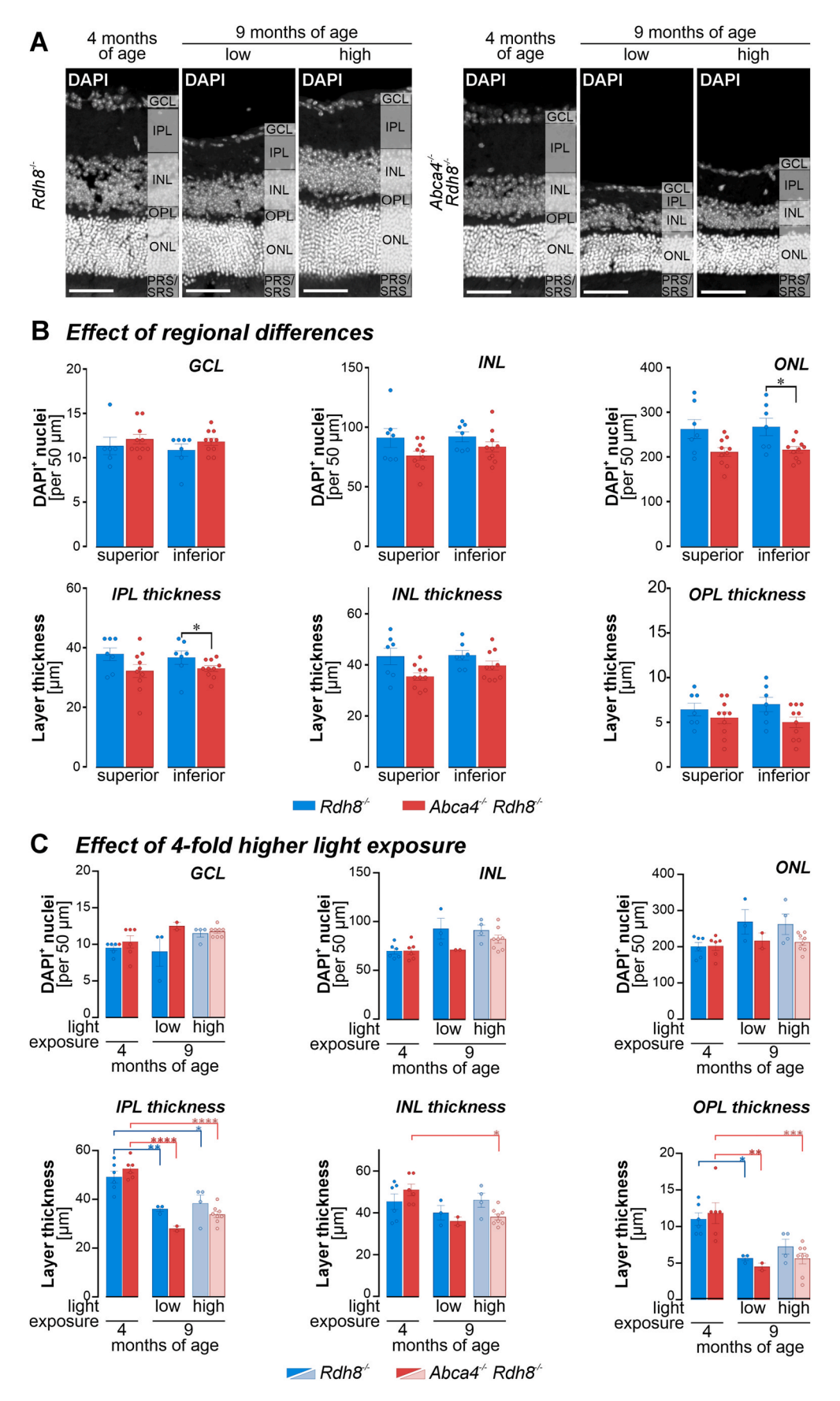
Fig. 1. RPE autofluorescence and microglial activation in 4- and 9-month-old  $Abca4^{-/-}$  Rdh8<sup>-/-</sup> double knockout compared to Rdh8<sup>-/-</sup> single knockout mice. A: Left, representative confocal microscopy images of autofluorescent (green) RPE flatmounts from animals kept under the indicated light conditions from age of 4 months onwards and as determined by using 488 nm laser excitation. Before 4 months of age, cage position and thus light exposure were not tracked. Scale bars,  $50 \mu m$ . Right, quantitative analysis of RPE autofluorescence. The bars represent mean values  $\pm$  SEM. A total of n=2–7 animals per genotype and age were analyzed. Each dot represents a biological replicate. Statistically significant differences were determined using the Mann-Whitney U test. \*P < 0.05. ADU: arbitrary digital unit. B: Left, Representative confocal microscopy images of immunofluorescence staining for the microglia marker IBA1 in central retinal flatmounts, focused on the inner plexiform layer (IPL), under the indicated conditions. Scale bars, 50 µm. Right, Quantification of IBA1<sup>+</sup> microglia per scan field (approximately 0.2 mm<sup>2</sup>; top). Bars represent mean values  $\pm$  SEM. A total of n = 2–7 animals per genotype, age and condition were analyzed. Each dot represents a biological replicate. Statistically significant differences according to the Mann-Whitney U test. \*P < 0.05. C: Quantification of subretinal IBA1+ microglia per central retinal section. Left, Representative images of retinal areas with and without a presumptive subretinal microglia (asterisk). Right, Quantitative data obtained from 9-month-old animals kept under bright light conditions. A total of n=4 animals per genotype was analyzed. Each dot represents a biological replicate. The Mann-Whitney U test was run for statistical testing. D: Morphometric analysis of microglial changes known to be associated with changes in the functional state including the size of their soma area (left) and the total area occupied by the processes of each microglial cell (right). A total of n = 38-208 IBA1+ cells from 2 to 7 animals per genotype, age and condition were analyzed for inner retinal layers, while much less microglia were found in the outer retina, determining the respective features in 10-22 cells per  $condition. \ Statistically \ significant \ differences \ according \ to \ an \ ordinary \ one-way \ ANOVA \ with \ multiple \ comparisons. \ ^*P < 0.05., \ ^***P < 0.001. \ ^***P < 0.0001. \ GCL: \ ^***P < 0.001. \ ^**P < 0.001. \ ^*P < 0.001$ ganglion cell layer; INL: inner nuclear layer; OPL: outer plexiform layer; ONL: outer nuclear layer; PRS: photoreceptor segments; SRS: subretinal space. (For interpretation of the references to colour in this figure legend, the reader is referred to the Web version of this article.)

areas (Maeda et al., 2008), we conducted a differential analysis of these retinal regions in 9-month-old animals including both nuclear and plexiform layers; inner retinal layers were examined as a control. We found a trend of 10-20 % fewer nuclei in the INL and ONL of the inferior, but also the superior, retina of *Abca4*<sup>-/-</sup> *Rdh8*<sup>-/-</sup> double knockout mice compared to Rdh8<sup>-/-</sup> single knockout mice that only reached significance levels for the ONL in the inferior subregion (Fig. 2B). Additionally, we studied the region-dependent changes in thicknesses of the individual retinal layers (Fig. 2B). Similar trends were also observed for these readouts, with a thinner inner plexiform layer (IPL), inner nuclear layer (INL) and outer plexiform layer (OPL) in *Abca4*<sup>-/-</sup> *Rdh8*<sup>-/-</sup> knockout mice compared to *Rdh8*<sup>-/-</sup> knockouts. However, only the difference in IPL thickness in the inferior retina was significant (Fig. 2B). In contrast to Maeda et al. (2008), we did not find overt regional differences regarding the progression of retinal degeneration in any of the applied readouts. The cross comparisons between superior and inferior regions did not reach significance levels. Several mouse models of retinal degeneration display hemispheric asymmetry in disease severity, with the inferior retina being particularly vulnerable in some contexts. For example, in C57BL/6J mice exposed to hyperoxia, photoreceptor loss begins at a locus ~0.5 mm inferior to the optic disc, coinciding with region-specific transcriptional changes (Zhu et al., 2010). Similarly, the Crb1^rd8/rd8 mutation, present in C57BL/6N substrains, produces focal inferior retinal dysplasia and degeneration, often with pseudorosettes (Mattapallil et al., 2012; Mehalow et al., 2003). It has been suggested that the more rapid disease progression in the inferior retina may be driven by differential light exposure, as the inferior retina receives more illumination due to most light sources being positioned in the superior visual field, thereby accelerating degeneration (Paskowitz et al., 2006). This seems to hold true for some murine models of retinal degeneration (Naash et al., 1996), but also for instance for patients suffering from retinitis pigmentosa (Heckenlively et al., 1991). However, this pattern is not universal across inherited retinal degeneration models and cell types: in rd1 mice, M/L-cones are better preserved superiorly while S-cones survive longer inferiorly (LaVail et al., 1997; Narayan et al., 2019). Recent spatial transcriptomics studies further suggest that regional gene-expression differences may underlie location-specific susceptibilities, which can vary by genotype, cell type, and environmental stress factors (Schumann et al., 2025). However, in the present study, we did not perform a photoreceptor subtype specific analysis. This question should be addressed in future studies potentially combined with functional readouts like electroretinogramm recordings to further pinpoint the phenotype of the *Abca4*<sup>-/-</sup> *Rdh8*<sup>-/-</sup> mice. All in all, we observed only few signs of neurodegeneration and microglial activation in our Abca4-/- Rdh8-/- strain that went beyond the age-related changes also observed in the single knockouts.

Enhanced neurodegeneration in response to acute light damage—specifically, a 30 to 60-min exposure to 10,000 lux in 4-week-old

 $Abca4^{-/-}$  Rdh8<sup>-/-</sup> mice lacking the rd8 mutation—has been previously reported (Maeda et al., 2014; Parmar et al. 2016, 2018; Schur et al., 2018; Yu et al., 2021). In this study, we investigated whether chronic, moderately (~4 fold) increased light exposure would influence the development of the otherwise mild phenotype observed in our double knockout strain. To test this, beginning at 4 months of age, a subgroup of mice was housed in cages on the top row of the racks, where light exposure inside the cages reached up to 190 lux, for a duration of 5 months. The control group remained on the bottom row, where light levels in the cages averaged  $\sim\!45$  lux. This experimental setup only revealed a significant age-related thinning of the plexiform layers in both genotypes (Fig. 2C). 9-Months-old Abca4<sup>-/-</sup> Rdh8<sup>-/-</sup> mice generally started to show slightly lower cell counts compared to Rdh8<sup>-/-</sup> mice, although these differences were not significant. Moreover, the relative reduction in plexiform layer thickness was more pronounced in the double knockouts—averaging 40-50 % of the values observed at 4 months—compared to approximately 30 % in Rdh8<sup>-/-</sup> mice. However, also this difference between genotypes did not reach statistical signifi-None of the investigated parameters showed genotype-dependent difference (Fig. 2C). This implies that the absence of both ABCA4 and RDH8, in the absence of the rd8 mutation, does not lead to an elevated susceptibility to this mild, chronic light stress model. Presumably, it needs much higher light intensities to elicit comparable effects as observed by others (Maeda et al., 2014; Parmar et al. 2016, 2018; Schur et al., 2018; Yu et al., 2021).

Overall, Abca4<sup>-/-</sup> Rdh8<sup>-/-</sup> double knockout mice on the C57BL/6J background, free of the confounding rd8 mutation, presented a limited retinal pathology and microglial activation profile when compared to Rdh8<sup>-/-</sup> single knockouts. The observed retinal changes included increased autofluorescence and specific minor alterations in retinal morphology. Despite these changes, the degree of retinal degeneration in the double knockout mice was less pronounced than anticipated based on previous reports. The discrepancies are likely due to the inbred rd8 mutation in the mixed C57BL/6N mouse strain studied in previous reports (Mehalow et al., 2003; Mattapallil et al., 2012), rather than the combined lack of ABCA4 and RDH8. Support for our observation of a much milder phenotype than initially described comes from Pan et al., (2021). They report a largely intact ONL in animals up to 30 months old, with significant disorganization occurring only near regions of extensive RPE shedding. Also, more recent studies from the Maeda lab investigate a double knockout genotype that should match the one we describe -Abca4-/- Rdh8-/- with RPE65 leucine variant, but free of the rd8 mutation (Kohno et al., 2014; Maeda et al., 2014; Palczewska et al., 2016). Both OCT analysis (Kohno et al., 2014) as well as electron microscopic images from the photoreceptor segments and part of the ONL (Palczewska et al., 2016) imply that in contrast to the earlier publications, there is a clearly maintained ONL as well as photoreceptor segments in 6 months old double knockout mice.



(caption on next page)

Fig. 2. Morphometric analysis of retinal integrity from  $Abca4^{-/-}$   $Rdh8^{-/-}$  double knockout mice compared to  $RDH8^{-/-}$  single knockout mice. A: Representative confocal microscopy images of DAPI staining in central retinal sections of the indicated conditions. Scale bars, 50  $\mu$ m. B: Comparison of indicated morphometric parameters from retinal sections collected ~200  $\mu$ m superior and inferior to the optic nerve in 9-month-old  $Abca4^{-/-}$   $Rdh8^{-/-}$  double knockout and  $Rdh8^{-/-}$  single knockout mice. C: Quantitative analysis of the same morphometric parameters as in B, discriminating 9-month-old animals exposed to high versus low light conditions. B and C: Bars represent mean values  $\pm$  SEM. A total of n=2-7 animals per genotype and age were analyzed – each dot represents the data from a single individual. Mann-Whitney U test. \*P < 0.05. \*\*P < 0.01. \*\*\*P < 0.001. GCL: ganglion cell layer, IPL: inner plexiform layer, INL: inner nuclear layer, OPL: outer plexiform layer, ONL: outer nuclear layer.

Note that this study focused solely on assessing the extent of neurodegeneration; other notable features of this murine Stargardt model—such as detailed characterization of the RPE phenotype beyond autofluorescent material accumulation, complement activation, drusen formation, and early neovascular changes—were beyond its scope. Here we refer the interested reader to recent studies (indirectly) addressing these aspects in  $Abca4^{-/-}$  Rdh8<sup>-/-</sup> double knockout mice free from the rd8 mutation (Kohno et al., 2014; Maeda et al., 2014; Parmar et al. 2016, 2018; Schur et al., 2018; Pan et al., 2021; Yu et al., 2021).

Our re-characterization of *Abca4*<sup>-/-</sup> *Rdh8*<sup>-/-</sup> double knockout mice revealed that a previously unrecognized confounding mutation in the Crb1 gene very likely was responsible for the major neurodegenerative phenotype including the peculiar inferior to superior pattern. This underscores the critical importance of rigorously controlling for genetic background and potential modifier genes in mouse models—though this of course is inherently constrained by the knowledge of the existence of such modifiers and their distribution across inbred strains. Furthermore, selecting Abca4<sup>-/-</sup> Rdh8<sup>-/-</sup> mice that lack the rd8 mutation may pose challenges for studies aiming to test therapeutic interventions targeting neurodegeneration, given the reduced severity of degeneration in the absence of this mutation even in animals 9 months of age. One way to address this issue would be to test animals at an older age. However, it is still necessary to verify the trend observed in our study suggesting that as age increases, phenotypes become more apparent, potentially leading to more significant neurodegeneration. Alternatively, Abca4<sup>-/-</sup> Rdh8<sup>-</sup> mice could be crossbreed with mice that express a third potential mechanism that leads to outer retinal pathology (e.g. as in (Kohno et al., 2014)). Finally, the animals could be exposed to additional stressors, such as light damage (Kohno et al., 2014; Maeda et al., 2014) or cigarette smoke (Fujihara et al., 2008), to enhance the phenotype. These approaches could also be used to model the multifactorial mechanisms that contribute to Stargardt disease and age-related macular degeneration, a condition in which genetic factors (including ABCA4 mutations), environmental factors, and age drive the pathology of the outer retina. Thus, Abca4<sup>-/-</sup> Rdh8<sup>-/-</sup> remain a valuable basis to develop model systems for research into Stargardt disease and age-related macular degeneration and treatment strategies.

## CRediT authorship contribution statement

**Sarah Glänzer:** Writing – review & editing, Writing – original draft, Visualization, Methodology, Investigation. **Josef Biber:** Validation, Supervision, Project administration, Methodology, Formal analysis, Conceptualization. **Antje Grosche:** Writing – review & editing, Visualization, Supervision, Resources, Project administration, Funding acquisition, Data curation, Conceptualization.

#### **Disclosures**

None.

# **Funding**

This project was supported by the Deutsche Forschungsgemeinschaft (grant DFG-GR 4403/2–1; GR 4403/5–1 to A.G.).

#### **Declaration of competing interest**

The authors declare the following financial interests/personal relationships which may be considered as potential competing interests: Antje Grosche reports financial support was provided by German Research Foundation. Antje Grosche reports a relationship with Elsevier - Executive Editor for Experimental Eye Research that includes: board membership. If there are other authors, they declare that they have no known competing financial interests or personal relationships that could have appeared to influence the work reported in this paper.

## Acknowledgements

We thank Gabriele Jäger for excellent technical support.

#### Data availability

Data will be made available on request.

#### References

- Allikmets, R., Singh, N., Sun, H., Shroyer, N.F., Hutchinson, A., Chidambaram, A., Gerrard, B., Baird, L., Stauffer, D., Peiffer, A., Rattner, A., Smallwood, P., Li, Y., Anderson, K.L., Lewis, R.A., Nathans, J., Leppert, M., Dean M Lupski, J.R., 1997. A photoreceptor cell-specific ATP-Binding transporter gene (ABCR) is mutated in recessive stargardt macualr dystrophy. Nat. Genet. 236–246.
- Arrigo, A., Cremona, O., Aragona, E., Casoni, F., Consalez, G., Dogru, R.M., Hauck, S.M., Antropoli, A., Bianco, L., Parodi, M.B., Bandello, F., Grosche, A., 2025. Muller cells trophism and pathology as the next therapeutic targets for retinal diseases. Prog. Retin. Eye Res. 106, 101357. https://doi.org/10.1016/j.preteyeres.2025.101357.
- Burke, T.R., Duncker, T., Woods, R.L., Greenberg, J.P., Zernant, J., Tsang, S.H., Smith, R. T., Allikmets, R., Sparrow, J.R., Delori, F.C., 2014. Quantitative fundus autofluorescence in recessive Stargardt disease. Investig. Ophthalmol. Vis. Sci. 55, 2841–2852. https://doi.org/10.1167/iovs.13-13624.
- Charbel Issa, P., Barnard, A.R., Singh, M.S., Carter, E., Jiang, Z., Radu, R.A., Schraermeyer, U., MacLaren, R., 2013. Fundus autofluorescence in the Abca4–/– mouse model of stargardt disease—correlation with accumulation of A2E, retinal function, and histology. Investig. Ophthalmol. Vis. Sci. 8, 5602–5612.
- Chen, Y., Okano, K., Maeda, T., Chauhan, V., Golczak, M., Maeda, A., Palczewski, K., 2012. Mechanism of all-trans-retinal toxicity with implications for Stargardt disease and age-related macular degeneration. J. Biol. Chem. 287, 5059–5069. https://doi. org/10.1074/jbc.M111.315432.
- Chen, Y., Palczewska, G., Mustafi, D., Golczak, M., Dong, Z., Sawada, O., Maeda, T., Maeda, A., Palczewski, K., 2013. Systems pharmacology identifies drug targets for stargardt disease-associated retinal degeneration. J. Clin. Investig. 123, 5119–5134. https://doi.org/10.1172/JCI69076.
- Choi, E.H., Daruwalla, A., Suh, S., Leinonen, H., Palczewski, K., 2021. Retinoids in the visual cycle: role of the retinal G protein-coupled receptor. J. Lipid Res. 62, 100040. https://doi.org/10.1194/jlr.TR120000850.
- Danciger, M., Matthes, M.T., Yasamura, D., Akhmedov, N.B., Rickabaugh, T., Gentleman, S., Redmond, T.M., La Vail, M.M., Farber, D.B., 2000. A QTL on distal chromosome 3 that influences the severity of light-induced damage to mouse photoreceptors. Mamm. Genome 11, 422–427. https://doi.org/10.1007/ s003350010081.
- Fujihara, M., Nagai, N., Sussan, T.E., Biswal, S., Handa, J.T., 2008. Chronic cigarette smoke causes oxidative damage and apoptosis to retinal pigmented epithelial cells in mice. PLoS One 3, e3119. https://doi.org/10.1371/journal.pone.0003119.
- Genead, M.A., Fishman, G.A., Stone Em Allikmets, R., 2009. The natural history of Stargardt disease with specific sequence mutation in the ABCA4 gene. Investig. Ophthalmol. Vis. Sci. 50, 5867–5871. https://doi.org/10.1167/jovs.09-3611.
- Heckenlively, J.R., Rodriguez, J.A., Daiger, S.P., 1991. Autosomal dominant sectoral retinitis pigmentosa. Two families with transversion mutation in codon 23 of rhodopsin. Arch. Ophthalmol. 109, 84–91. https://doi.org/10.1001/ archopht.1991.01080010086038.
- Jabri, Y., Biber, J., Diaz-Lezama, N., Grosche, A., Pauly, D., 2020. Cell-type-specific complement profiling in the ABCA4(-/-) mouse model of Stargardt disease. Int. J. Mol. Sci. 21. https://doi.org/10.3390/ijms21228468.

- Katz, M.L., Redmond, T.M., 2001. Effect of Rpe65 knockout on accumulation of lipofuscin fluorophores in the retinal pigment epithelium. Investig. Ophthalmol. Vis. Sci. 42 (12), 3023–3030. PMID: 11687551.
- Kim, S.R., Fishkin, N., Kong, J., Nakanishi, K., Allikmets, R., Sparrow, J.R., 2004. Rpe65 Leu450Met variant is associated with reduced levels of the retinal pigment epithelium lipofuscin fluorophores A2E and iso-A2E. Proc. Natl. Acad. Sci. U. S. A. 101. 11668–11672. https://doi.org/10.1073/pnas.0403499101.
- Kiser, P.D., Golczak, M., Palczewski, K., 2014. Chemistry of the retinoid (visual) cycle. Chem. Rev. 114, 194–232. https://doi.org/10.1021/cr400107q.
- Kohno, H., Maeda, T., Perusek, L., Pearlman, E., Maeda, A., 2014. CCL3 production by microglial cells modulates disease severity in murine models of retinal degeneration. J. Immunol. 192, 3816–3827. https://doi.org/10.4049/jimmunol.1301738.
- LaVail, M.M., Matthes, M.T., Yasumura, D., Steinberg, R.H., 1997. Variability in rate of cone degeneration in the retinal degeneration (rd/rd) mouse. Exp. Eye Res. 65, 45–50. https://doi.org/10.1006/exer.1997.0308.
- Maeda, A., Maeda, T., Golczak, M., Palczewski, K., 2008. Retinopathy in mice induced by disrupted all-trans-retinal clearance. J. Biol. Chem. 283, 26684–26693. https://doi. org/10.1074/jbc.M804505200.
- Maeda, A., Palczewska, G., Golczak, M., Kohno, H., Dong, Z., Maeda, T., Palczewski, K., 2014. Two-photon microscopy reveals early rod photoreceptor cell damage in lightexposed mutant mice. Proc. Natl. Acad. Sci. U. S. A. 111, E1428–E1437. https://doi. org/10.1073/pnas.1317986111.
- Maeda, A., Maeda, T., Golczak, M., Chou, S., Desai, A., Hoppel, C.L., Matsuyama, S., Palczewski, K., 2009. Involvement of all-trans-retinal in acute light-induced retinopathy of mice. J. Biol. Chem. 284, 15173–15183. https://doi.org/10.1074/jbc. M900322200.
- Mattapallil, M.J., Wawrousek, E.F., Chan, C.C., Zhao, H., Roychoudhury, J., Ferguson, T. A., Caspi, R.R., 2012. The Rd8 mutation of the Crb1 gene is present in vendor lines of C57BL/6N mice and embryonic stem cells, and confounds ocular induced mutant phenotypes. Investig. Ophthalmol. Vis. Sci. 53, 2921–2927. https://doi.org/10.1167/joys.12-9662
- Mehalow, A.K., Kameya, S., Smith, R.S., Hawes, N.L., Denegre, J.M., Young, J.A., Bechtold, L., Haider, N.B., Tepass, U., Heckenlively, J.R., Chang, B., Naggert, J.K., Nishina, P.M., 2003. CRB1 is essential for external limiting membrane integrity and photoreceptor morphogenesis in the Mammalian retina. Hum. Mol. Genet. 12, 2179–2189. https://doi.org/10.1093/hmg/ddg232.
- Molday, L.L., Rabin, A.R., Molday, R.S., 2000. ABCR expression in foveal cone photoreceptors and its role in stargardt macular dystrophy. Nat. Genet. 25, 257–258. https://doi.org/10.1038/77004.
- Molday, L.L., Wahl, D., Sarunic, M.V., Molday, R.S., 2018. Localization and functional characterization of the p.Asn965Ser (N965S) ABCA4 variant in mice reveal pathogenic mechanisms underlying stargardt macular degeneration. Hum. Mol. Genet. 27, 295–306. https://doi.org/10.1093/hmg/ddx400.
- Naash, M.L., Peachey, N.S., Li, Z.Y., Gryczan, C.C., Goto, Y., Blanks, J., Milam, A.H., Ripps, H., 1996. Light-induced acceleration of photoreceptor degeneration in transgenic mice expressing mutant rhodopsin. Investig. Ophthalmol. Vis. Sci. 37, 277.
- Narayan, D.S., Ao, J., Wood, J.P.M., Casson, RJ.Chidlow G., 2019. Spatio-temporal characterization of S- and M/L-cone degeneration in the Rd1 mouse model of retinitis pigmentosa. BMC Neurosci. 20, 46. https://doi.org/10.1186/s12868-019-0528-2
- Palczewska, G., Maeda, A., Golczak, M., Arai, E., Dong, Z., Perusek, L., Kevany, B., Palczewski, K., 2016. Receptor MER tyrosine kinase proto-Oncogene (MERTK) is not required for transfer of bis-retinoids to the retinal pigmented epithelium. J. Biol. Chem. 291, 26937–26949. https://doi.org/10.1074/jbc.M116.764563.
- Pan, C., Banerjee, K., Lehmann, G.L., Almeida, D., Hajjar, K.A., Benedicto, I., Jiang, Z., Radu, R.A., Thompson, D.H., Rodriguez-Boulan, E., Nociari, M.M., 2021. Lipofuscin causes atypical necroptosis through lysosomal membrane permeabilization. Proc. Natl. Acad. Sci. U. S. A. 118. https://doi.org/10.1073/pnas.2100122118.
- Paolicelli, R.C., Sierra, A., Stevens, B., Tremblay, M.E., Aguzzi, A., Ajami, B., Amit, I., Audinat, E., Bechmann, I., Bennett, M., Bennett, F., Bessis, A., Biber, K., Bilbo, S., Blurton-Jones, M., Boddeke, E., Brites, D., Brone, B., Brown, G.C., Butovsky, O., Carson, M.J., Castellano, B., Colonna, M., Cowley, S.A., Cunningham, C., Davalos, D., De Jager, P.L., de Strooper, B., Denes, A., Eggen, B.J.L., Eyo, U., Galea, E., Garel, S., Ginhoux, F., Glass, C.K., Gokce, O., Gomez-Nicola, D., Gonzalez, B., Gordon, S., Graeber, M.B., Greenhalgh, A.D., Gressens, P., Greter, M., Gutmann, D.H., Haass, C., Heneka, M.T., Heppner, F.L., Hong, S., Hume, D.A., Jung, S., Kettenmann, H., Kipnis, J., Koyama, R., Lemke, G., Lynch, M., Majewska, A., Malcangio, M., Malm, T., Mancuso, R., Masuda, T., Matteoli, M.,

- McColl, B.W., Miron, V.E., Molofsky, A.V., Monje, M., Mracsko, E., Nadjar, A., Neher, J.J., Neniskyte, U., Neumann, H., Noda, M., Peng, B., Peri, F., Perry, V.H., Popovich, P.G., Pridans, C., Priller, J., Prinz, M., Ragozzino, D., Ransohoff, R.M., Salter, M.W., Schaefer, A., Schaefer, D.P., Schwartz, M., Simons, M., Smith, C.J., Streit, W.J., Tay, T.L., Tsai, L.H., Verkhratsky, A., von Bernhardi, R., Wake, H., Wittamer, V., Wolf, S.A., Wu, L.J., Wyss-Coray, T., 2022. Microglia states and nomenclature: a field at its crossroads. Neuron 110, 3458–3483. https://doi.org/10.1016/j.neuron.2022.10.020.
- Parmar, T., Parmar, V.M., Arai, E., Sahu, B., Perusek, L., Maeda, A., 2016. Acute stress responses are early molecular events of retinal degeneration in Abca4-/-Rdh8-/mice after light exposure. Investig. Ophthalmol. Vis. Sci. 57, 3257–3267. https://doi. org/10.1167/jovs.15-18993.
- Parmar, T., Parmar, V.M., Perusek, L., Georges, A., Takahashi, M., Crabb, J.W., Maeda, A., 2018. Lipocalin 2 plays an important role in regulating inflammation in retinal degeneration. J. Immunol. 200, 3128–3141. https://doi.org/10.4049/ immunol.1701573.
- Paskowitz, D.M., LaVail, M.M., Duncan, J.L., 2006. Light and inherited retinal degeneration. Br. J. Ophthalmol. 90 (8), 1060–1066. https://doi.org/10.1136/bjo.2006.097436. Epub 2006 May 17. PMID: 16707518; PMCID: PMC1857196.
- Radu, R.A., Hu, J., Yuan, Q., Welch, D.L., Makshanoff, J., Lloyd, M., McMullen, S., Travis, G.H., Bok, D., 2011. Complement system dysregulation and inflammation in the retinal pigment epithelium of a mouse model for stargardt macular degeneration. J. Biol. Chem. 286, 18593–18601. https://doi.org/10.1074/jbc.M110.191866.
- Rudolph, G., Kalpadakis, P., Haritoglou, C., Rivera, A., Weber, B.H.F., 2002. Mutationen im ABCA4-Gen in einer Familie mit Stargardtscher Erkrankung und Retinitis pigmentosa (STGD1/RP19). Klin. Monatsblätter Augenheilkd. 8, 590–596.
- Schindelin, J., Arganda-Carreras, I., Frise, E., Kaynig, V., Longair, M., Pietzsch, T., Preibisch, S., Rueden, C., Saalfeld, S., Schmid, B., Tinevez, J.Y., White, D.J., Hartenstein, V., Eliceiri, K., Tomancak, P., Cardona, A., 2012. Fiji: an open-source platform for biological-image analysis. Nat. Methods 9, 676–682. https://doi.org/10.1038/nneth.2019.
- Schumann, U., Liu, L., Aggio-Bruce, R., Cioanca, A.V., Shariev, A., Madigan, M.C., Valter, K., Wen, J., Natoli, R., 2025. Spatial transcriptomics reveals regionally altered gene expression that drives retinal degeneration. Commun. Biol. 8, 629. https://doi.org/10.1038/s42003-025-07887-2.
- Schur, R.M., Gao, S., Yu, G., Chen, Y., Maeda, A., Palczewski, K., Lu, Z.R., 2018. New GABA modulators protect photoreceptor cells from light-induced degeneration in mouse models. FASEB J. 32, 3289–3300. https://doi.org/10.1096/fi.201701250R.
- Shiose, S., Chen, Y., Okano, K., Roy, S., Kohno, H., Tang, J., Pearlman, E., Maeda, T., Palczewski, K., Maeda, A., 2011. Toll-like receptor 3 is required for development of retinopathy caused by impaired all-trans-retinal clearance in mice. J. Biol. Chem. 286, 15543–15555. https://doi.org/10.1074/jbc.M111.228551.
- Stargardt, K., 1909. Über familiäre, progressive Degeneration in der Maculagegend des Auges. Graefe's Arch. Ophthalmol. 534–550.
- Stargardt, K., 1913. I. Über familiäre, progressive Degeneration in der Maculagegend des Auges. Zeitschrift für Augenheilkunde 95–116.
- Stargardt, K., 1916. IV. Zur Kasuistik der "Familiären, progressiven Degeneration in der Maculagegend des Auges. Zeitschrift für Augenheilkunde 249–255.
- Stence, N., Waite, M., Dailey, M.E., 2001. Dynamics of microglial activation: a confocal time-lapse analysis in hippocampal slices. Glia 33, 256–266.
- Sun, H., Nathans, J., 1997. Stargardt's ABCR is localized to the disc membrane of retinal rod outer segments. Nat. Genet. 17, 15–16. https://doi.org/10.1038/ng0997-15.
- Walker, F.R., Nilsson, M., Jones, K., 2013. Acute and chronic stress-induced disturbances of microglial plasticity, phenotype and function. Curr. Drug Targets 14, 1262–1276. https://doi.org/10.2174/13894501113149990208.
- Wenzel, A., Reme, C.E., Williams, T.P., Hafezi, F.Grimm C., 2001. The Rpe65 Leu450Met variation increases retinal resistance against light-induced degeneration by slowing rhodopsin regeneration. J. Neurosci. 21, 53–58. https://doi.org/10.1523/ JNFUROSCI.21-01-00053\_2001.
- Wu, L., Nagasaki, T., Sparrow, J., 2010. Photoreceptor cell degeneration in Abcr—/—mice. Adv. Exp. Med. Biol. 664, 533–539.
- Yu, G., Gao, S.Q., Dong, Z., Sheng, L., Sun, D., Zhang, N., Zhang, J., Margeivicus, S., Fu, P., Golczak, M., Maeda, A., Palczewski, K., Lu, Z.R., 2021. Peptide derivatives of retinylamine prevent retinal degeneration with minimal side effects on vision in mice. Bioconjug. Chem. 32, 572–583. https://doi.org/10.1021/acs.bioconjchem.1c00043.
- Zhu, Y., Natoli, R., Valter, K., Stone, J., 2010. Differential gene expression in mouse retina related to regional differences in vulnerability to hyperoxia. Mol. Vis. 16, 740–755. PMID: 20454693; PMCID: PMC2862240.